coatings

MDPI

Article

Preparation of Hydrophilic and Fire-Resistant Phytic Acid/Chitosan/Polydopamine-Coated Expanded Polystyrene Particles by Using Coating Method

Wenjie Tang, Dajian Huang *, Xiaohu Qiang and Wang Liu

School of Materials Science and Engineering, Lanzhou Jiaotong University, Lanzhou 730070, China; tangwenjie2019@163.com (W.T.); qiangxh2018@126.com (X.Q.); ssliuwang@163.com (W.L.)
* Correspondence: huangdj2015@yeah.net; Tel.: +86-931-4956-651

Abstract: Expanded polystyrene (EPS) particles are commonly used for thermal insulation in lightweight building materials due to their low density, low thermal conductivity, and affordability. However, shortcomings such as hydrophobicity and poor fire safety limit the application of EPS. Bio-based flame retardants have been developed for use in polymer composites due to their renewable, environmentally friendly, and non-toxic properties. In this study, to improve the hydrophilicity and fire resistance of EPS particles, phytic acid (PA)/chitosan (CS)–polydopamine (PDA)@EPS particles (PA/CS-PDA@EPS) with a bio-based coating were prepared by using a simple coating method based on PDA@EPS particles using PDA as an adhesive and PA and CS as bio-based flame retardants. The results showed that the modified EPS particles had good hydrophilicity, the residual carbon yield of the 10PA/3CS-PDA@EPS samples was increased to 24 wt%, and the maximum loss rate was reduced by 69% compared with unmodified EPS. In flammability tests, the 10PA/3CS-PDA@EPS samples also demonstrated low flame spread and some fire resistance. Furthermore, the modified EPS particles exhibited fire resistance even after multiple washings. The hydrophilic and fire-resistant modified EPS particles are anticipated to offer a novel approach to the advancement of EPS-based lightweight building materials.

Keywords: bio-based coating; expanded polystyrene particles; bio-based flame retardant

Citation: Tang, W.; Huang, D.; Qiang, X.; Liu, W. Preparation of Hydrophilic and Fire-Resistant Phytic Acid/Chitosan/Polydopamine-Coated Expanded Polystyrene Particles by Using Coating Method. *Coatings* **2024**, *14*, 574. https://doi.org/10.3390/coatings14050574

Academic Editors: Simona Căprărescu and Cristina Modrogan

Received: 8 April 2024
Revised: 30 April 2024
Accepted: 2 May 2024
Published: 6 May 2024

1. Introduction

With the increase in global energy consumption, energy conservation and emission reduction has become a major concern. Studies show that energy consumption in buildings accounts for 32% of total energy consumption [1]. The thermal energy consumption of a building's external walls constitutes a significant portion of the overall building energy consumption [2]. To address this issue, lightweight building materials can be created during construction by adding a foaming agent [3,4] or lightweight aggregates [4,5] to the matrix material. This improves the thermal insulation capacity of the wall structure, resulting in reduced energy consumption [6]. Expanded polystyrene (EPS) particles are commonly used for thermal insulation in lightweight building materials due to their low density, low thermal conductivity, and affordability [7–9]. However, EPS, a porous polyolefin material, is highly flammable because of its hydrocarbon-rich main chain, numerous aromatic rings in the side chain, and high air circulation within the honeycomb structure [10,11]. Furthermore, the hydrophobicity of EPS causes the EPS particles to float and be unevenly dispersed in the slurry, and the hydration products of inorganic materials are difficult to penetrate. This poor interface between EPS particles and matrix materials often renders EPS particles a weak link in the system, compromising the comprehensive performance of lightweight building materials [9,12]. Therefore, it is necessary to implement effective modification measures to improve the hydrophilicity and fire resistance of EPS in the production of lightweight building materials.

The addition of flame retardants in the polymerization or impregnation process of EPS is an effective way to obtain flame retarded EPS. However, these methods have a large limitation on the particle size of the flame retardants and there are some problems such as unpolymerized monomer residues and low impregnation efficiency [13,14]. The attachment of gels [15,16], aerogels [17], hydrogel [18], foams [19], films [20], and gelatinized materials [21] with flame-retardant properties to the surface of polymers represents an effective method for enhancing the fire resistance of polymers. The coating method, by coating each EPS particle surface with an adhesive and flame-retardant, is a good flame-retardant modification method [22,23]. Cao et al. [24] used aluminum nitrate-modified multi-walled carbon nanotubes (ATH-MWNTs) and expandable graphite (EG) for EPS flame-retardant modification using melamine-modified urea formaldehyde resin (MUF) as an adhesive with the encapsulation method. The modified EPS foams achieved a limiting oxygen index (LOI) of 30.3% and a UL-94 rating of V-0 when 14.3 wt% EG and 4.1 wt% ATH-MWNTs were added, and the peak of the heat release rate (pHRR) was reduced from 933 to 177 kW/m^2. Wang et al. [25] developed a cost-effective flame-retardant system for EPS foams using thermosetting phenolic resin (PF) as an adhesive and the high SiO_2 content of fly ash (FA) synergistic with ATH. In addition, for the EPS-PF/ATH35/FA15 sample with an EPS/PF/ATH/FA ratio of 50:50:35:15, the LOI was increased to 29.6%, and a UL-94 V-0 rating was achieved. However, the most commonly used adhesive for the coating method is thermosetting resins such as phenolic resins and melamine–formaldehyde resins. These resins often contain formaldehyde, which is harmful to human health [26]. Therefore, it is essential to choose an environmentally friendly, non-toxic, and flame-retardant adhesive.

Halogenated flame retardants are gradually being replaced due to the toxic substances released during combustion which are hazardous to human health and the environment [27,28]. Phosphorus-based flame retardants are halogen-free flame retardants of high efficiency and low toxicity [29,30], such as red phosphorus [31], aluminum hypophosphite [32], ammonium polyphosphate [33], and diammonium phosphate [34], which have been used for the flame-retardant modification of EPS. In the combustion process, the phosphorus-based flame retardant fulfils two main roles: (i) as a solid-phase flame retardant, it promotes carbon formation in oxygenated polymers; (ii) as a gas-phase flame retardant, it generates reactive radicals that remove H· and OH [29,35]. Nitrogen-based flame retardants are primarily composed of dicyandiamide [36], guanidine salt [37], melamine [38], and melamine salts [39]. During the combustion process, nitrogen-based flame retardants decompose and release inert gases (N_2, NH_3, and water vapor), thus acting as gas-phase flame retardants [35]. Nevertheless, nitrogen-based flame retardants exhibit low flame retardant efficiency and frequently necessitate the use of phosphorus-based flame retardants in conjunction with them [39–41]. Ji et al. [22] synthesized ammonium starch phosphate starch carbamate (APSC) using starch, phosphoric acid, and urea as raw materials. When the APCS content reached 47 wt%, the LOI of the modified EPS foams increased to 35.2% and achieved a V-0 rating of UL-94, with a significant reduction in pHRR and total smoke production (TSP). However, these flame retardants are non-renewable and non-degradable and possess a certain degree of biotoxicity [42].

Many bio-based flame retardants have been developed for use in polymer composites due to their renewable, environmentally friendly, and non-toxic properties [43,44], such as chitosan (CS) [45,46], phytic acid (PA) [47,48], alginate [49,50], and polydopamine (PDA) [51,52]. Mussel-inspired PDA is applied to the surface of all materials by spontaneous deposition, and the catechol groups in PDA provide excellent adhesion at the interface of organic and inorganic materials [53–58]. This allows PDA to be used as an adhesive. PA is myo-inositol hexaphosphate, which is solubilized in grains, nuts, legumes, and oilseeds by acidic, heat, ultrasonic irradiation, and enzymatic treatments, and precipitated as phytates through acidic dissociation [59–62]. PA contains 28 wt% elemental phosphorus and six phosphate groups. It can serve as an acid source in intumescent flame retardant (IFR) systems, producing phosphates during combustion [63,64]. This promotes the formation of phosphorus-rich char layers and breaks down volatile phosphides to trap

free radicals, inhibiting polymer combustion. In addition, PA can form complexes with positively charged polymers and metal ions (pKa 1.9~9.5) due to its high negative charge, which is carried by six phosphate groups [65]. CS is a non-toxic, highly productive, and environmentally friendly linear aminopolysaccharide produced from chitin in the shells of crustaceans (e.g., shrimps, crabs, and shells) through decalcification with acid treatment and partial deacetylation with alkali treatment [66,67]. CS consists of β(1-4)-linked D-glucosamine and low amounts of N-acetyl-β-D-glucosamine [68,69]. CS is a carbon-rich aminopolysaccharide that releases ammonia and forms residual carbon during thermal decomposition which can be used as a source of charcoal and gas [70]. PA and CS can form an IFR system that exhibits P-N synergistic flame retardancy. At low pH (pKa 6~6.5), CS carries a positive charge [71], and complex deposition takes place due to strong ionic interactions between negatively charged PA and positively charged CS [63]. Cheng et al. [72] used a layer-by-layer assembly method to introduce PA, biochar, and CS into cotton fabrics. The results demonstrated that the cotton fabric treated with PA/CS/BC (7.5%) exhibited an 88.66% reduction in pHRR and an 88.69% reduction in total heat release (THR), and the LOI was up to 64.1%. After being washed, the treated cotton retained about 60% of flame-retardant properties. Fang et al. [73] used the LbL assembly method to prepare polyester/cotton blend fabrics with PA/CS coatings, when PA/CS was 20 BL, the LOI was increased to 29.6%. Additionally, the phosphate groups, hydroxyl groups, and amino groups in PA and CS can increase the hydrophilicity of EPS [74,75]. Therefore, modification with PA/CS bio-based flame retardants can produce hydrophilic and flame-retardant EPS particles. However, there are no reports on bio-based PA/CS coatings that improve the fire resistance and hydrophilicity of EPS particles.

At present, the flame-retardant modification of expanded polystyrene (EPS) is primarily focused on EPS foam insulation boards. However, there are relatively few studies conducted on EPS particles. In the context of lightweight building materials, EPS is predominantly employed as a lightweight aggregate in the form of particles. Therefore, it is necessary to study the modification of EPS particles. In this study, a simple approach is proposed to enhance the fire resistance and hydrophilicity of EPS particles through the use of PA/CS bio-based coatings. A PA/CS of the IFR system was constructed on PDA@EPS particles using PDA as the adhesive, and PA/CS-PDA@EPS particles were produced by the simple coating method. The effect of the modified coating on the structure, hydrophilicity, thermal stability, and fire resistance of the EPS particles was investigated by relevant characterization. The prepared modified EPS particles are hydrophilic and fire resistant, which provides a certain reference value for the application of EPS particles.

2. Materials and Methods

2.1. Materials

The expanded polystyrene (EPS) particles had a bulk density of 11 kg/m^3 and their particle size was 3–5 mm. Dopamine hydrochloride (DA) was purchased from Aladdin. Tris(hydroxymethyl)aminomethane (Tris) was commercially available in analytical grade purchased from Zhongqin Chemical Reagent Co Ltd., Shanghai, China. The CS (deacetylation degree: 80~95%), hydrochloric acid (HCl, AR, 36.0~38.0%), and acetic acid were purchased from Sinopharm Chemical Reagent Co., Ltd., Shanghai, China. The PA (70% aqueous solution) was purchased from McLean Biochemical Technology Co., Ltd., Shanghai, China.

2.2. Preparation of Modified EPS Particles

2.2.1. Preparation of PDA-Coated Modified EPS Particles

Figure 1 shows the preparation process of modified EPS particles. Firstly, 1.21 g of Tris was dissolved in 1000 mL of deionized water and titrated with HCl to prepare a Tris-HCl buffer solution with pH = 8.5. A 4 mg/mL solution of Da was then prepared using a Tris-HCl buffer solution (10 mM, pH 8.5). The unmodified EPS particles were stirred continuously in the Da solution for 24 h. The EPS particles were rinsed with distilled

water until the solution became colorless and then dried in an oven at 40 °C. The resulting PDA-coated modified EPS particles were noted as PDA@EPS.

2.2.2. Preparation of CS-Modified PDA@EPS Particles

Firstly, 10 g of CS powder was added to 1000 mL of deionized water in a beaker and stirred for 3 min to disperse the powder. Then, 10 mL (1%) of acetic acid was added and stirred continuously for 24 h to produce a 1% (*w*/*v*) CS solution, which was recorded as 1% CS. Following the same method, 2% and 3% CS solutions were prepared. Then, the PDA@EPS particles were stirred in 1%, 2%, and 3% CS solutions for 3 h, fished out, and dried to produce 1CS-PDA@EPS, 2CS-PDA@EPS, and 3CS-PDA@EPS particles, respectively.

2.2.3. Preparation of PA/CS-Modified PDA@EPS Particles

Firstly, 28.57 g of PA (70%) solution was weighed and transferred to a beaker containing 1000 mL of deionized water and the mixture was stirred for 1 h to prepare a PA solution with a concentration of 2% (*w*/*v*). The pH of the PA solution was neutralized to 6 with a specific NaOH solution and stirred to obtain a 2% (*w*/*v*) PA-Na solution, designated as 2% PA. Similarly, 6% and 10% PA solutions were prepared. Then, the CS-PDA@EPS particles were stirred in different PA solutions for 3 h, retrieved, and dried. The modified particles were noted as 2PA/3CS-PDA@EPS, 6PA/3CS-PDA@EPS, and 10PA/3CS-PDA@EPS, respectively, based on the concentration of the PA solutions.

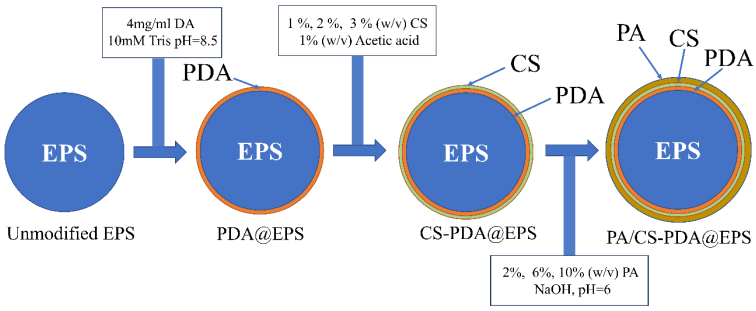

Figure 1. A schematic diagram of the modified EPS particle preparation process.

2.3. Characterizations

The microscopic morphology of various modified EPS particles was studied using a scanning electron microscope (SEM, ZEISS GeminiSEM 500, Carl Zeiss AG, Oberkochen, Germany) with an Oxford UltimMax 65 EDS energy spectrometer.

The hydrophilicity of the modified EPS particles was assessed by measuring the water contact angle (WCA) using a contact angle meter (OCA25, Eastern Dataphy Instruments Co., Beijing, China). The EPS foam board samples were cut to specifications of 4 cm × 4 cm × 2 cm. The same modification method as that used for the EPS particles was employed to prepare the modified EPS foam board samples. Subsequently, 5 μL of ultrapure water was dropped onto the surface of the modified EPS foam board samples, and the WCA was then measured.

The thermal stability of the modified EPS particles was studied using a TA TGA55 thermogravimetric analyzer (TA Instruments Co., Newcastle, DE, USA) through thermogravimetric analysis (TGA). A total of 4 mg of the sample was weighed into a crucible and heated from room temperature to 800 °C at a rate of 10 °C/min in a nitrogen atmosphere with a flow rate of 10 mL/min.

The flammability of the modified EPS particles was tested by using a butane flame combustion test. This test was similar to the test used in previous studies by Liu et al. [76], Xu et al. [77], and Chen et al. [78]. The butane gun was positioned at a distance of 8 cm from the sample, while the blue flame was about 3 cm, and the total flame was about 10 cm. In the flammability test, 100 cm^3 of EPS particles was stacked in a metal container and directly exposed to a butane flame to compare the changes during combustion.

The water resistance of the modified EPS pellets was assessed by washing them several times in tap water with agitation and recording the change in mass before and after.

3. Results

3.1. Morphology and Coating Efficiency

The morphology of unmodified EPS particles and coated modified EPS particles was analyzed by SEM and is shown in Figure 2. The surface of unmodified EPS particles is rough and has many holes, which are the result of the evaporation of the pentane blowing agent [79]. After the PDA-coating modification, the surface of the PDA@EPS particles is covered with a flat coating (Figure 2b). The PDA coating on the EPS surface serves as an adhesive, and the strong interaction between PDA and CS allows the CS to adhere to it [58]. The CS-PDA@EPS particles are prepared by coating CS onto the surface of PDA@EPS particles using the coating method. The apparent morphology of the particles is shown in Figure 2c–e. During film growth and adsorption, CS is a polysaccharide with a considerable hardness that can hinder the process and lead to island growth [65]. Aggregates are visible on the surface of the CS film, which should be the residue of island growth (Figure 2c). As the concentration of CS increases, the residue of the island on the surface of the modified EPS gradually disappears, and a flat and dense CS film is formed. The CS film on the surface of 1CS-PDA@EPS appears relatively flat. However, due to the spherical surface of EPS particles, it is difficult to achieve uniform film formation with high concentrations of CS solutions, resulting in the formation of folds and grooves. In addition, CS has excellent film formation and flexibility, and no significant cracks are found in all of the films [63].

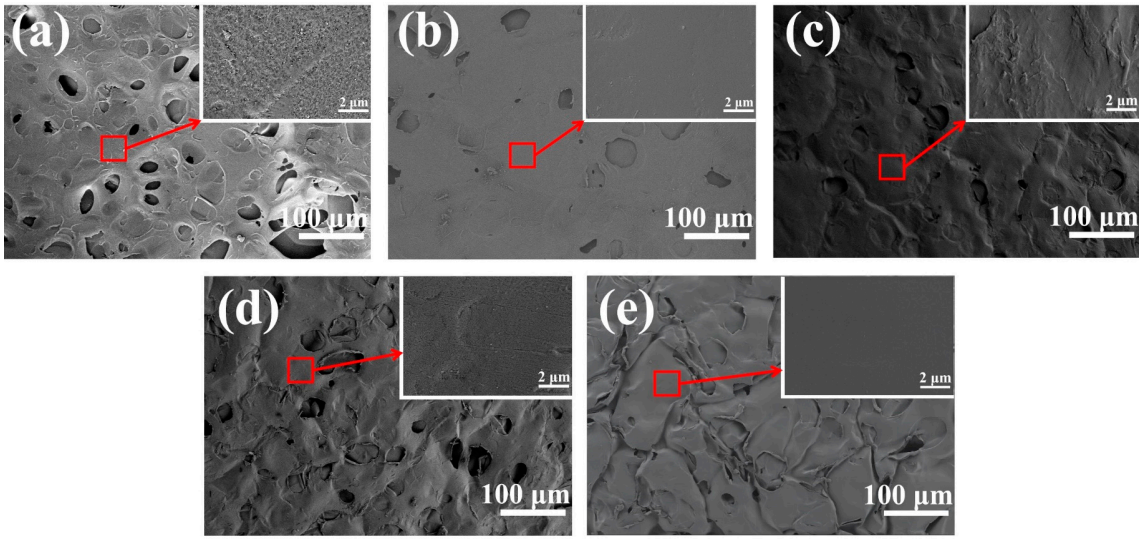

Figure 2. SEM images of EPS (**a**), PDA@EPS (**b**), 1CS-PDA@EPS (**c**), 2CS-PDA@EPS (**d**), and 3CS-PDa@EPS (**e**).

As indicated in Table 1, the high concentration of the CS solution promotes the growth of the CS films, which increases the coating efficiency. However, if the concentration of CS exceeds 3%, the solution's viscosity becomes too high for the application, and the dried modified EPS particles become bonded together and difficult to separate. The IFR system utilizes CS as a carbon and gas source. Therefore, EPS particles modified with CS, which has a high coating efficiency, will exhibit better thermal stability. For subsequent tests, 3CS-PDA@EPS particles will be used.

Figure 3 shows the morphology of the modified EPS particles at different PA concentrations. The strong ion–ion interaction between PA and CS results in the formation of a dense PA/CS coating on the PDA@EPS particles through complexation and deposition [65,80]. This process effectively eliminates the grooves on the surface of 3CS-PDA@EPS particles. Delamination of the coatings is observed in Figure 3b4, which is attributed to the low PA

concentration and incomplete complexation of the underlying CS. With the increase in PA concentration, PA and CS are fully complexed on the modified EPS surface and the surface coatings show a wrinkled morphology; the thickness of the coatings is increased significantly from 2.83 µm (1CS-PDA@EPS) to 6.46 µm (6PA/3CS-PDA@EPS) and 9.23 µm (10PA/3CS-PDA@EPS), respectively, and no obvious delamination between the coatings is found. Therefore, it can be assumed that an increase in PA concentration will cause more PA to attach to the surface of the modified EPS particles and increase the thickness of the surface coating. In addition, the convex aggregates present on the coating surface are associated with the island growth of chitosan and the complexation deposition with PA/CS. As shown in Table 1, the mass of 3CS-PDA@EPS is increased from 8 g to 9.27 g (15.9%), 10.38 g (29.77%), and 11.16 g (39.45%), respectively, with increasing PA concentration. The alteration in the mass of modified EPS particles indicates the successful complexation and deposition of PA/CS coatings.

Table 1. Coating efficiency of different modified EPS particles.

Sample	Initial Weight (g)	Final Weight (g) after Drying	Weight of Materials Coated on EPS (g)/Efficiency
PDA@EPS	8	8.22	0.22 (2.75%)
1CS-PDA@EPS	8	8.47	0.47 (5.91%)
2CS-PDA@EPS	8	9.48	1.48 (18.54%)
3CS-PDA@EPS	8	10.29	2.29 (28.58%)
2PA/3CS-PDA@EPS	8	9.27	1.27 (15.9%)
6PA/3CS-PDA@EPS	8	10.38	2.38 (29.77%)
10PA/3CS-PDA@EPS	8	11.16	3.16 (39.45%)

The mass calculation was carried out after drying.

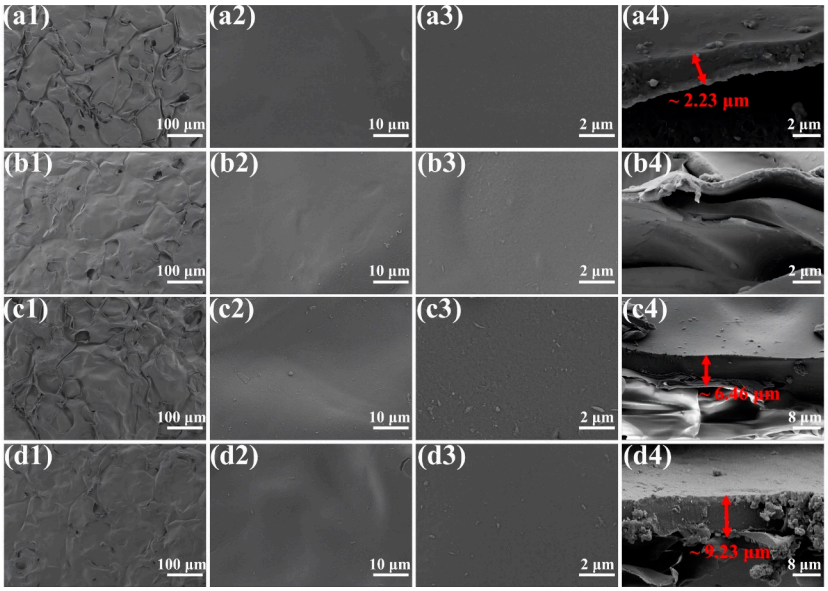

Figure 3. SEM images of 3CS-PDA@EPS (**a1**–**a4**), 2PA/3CS-PDA@EPS (**b1**–**b4**), 6PA/3CS-PDA@EPS (**c1**–**c4**), and 10PA/3CS-PDA@EPS (**d1**–**d4**).

3.2. FTIR Analyses of EPS Samples

The FTIR spectra of EPS samples are shown in Figure 4. The absorption peaks of unmodified EPS at 698 and 755 cm^{-1} correspond to aromatic C-H bending vibration, the bands at 1449 and 1492 cm^{-1} are assigned to C=C stretching vibration in the aromatic ring [55,81]. The absorption peaks at 2849 and 2920 cm^{-1} correspond to the symmetric and asymmetric stretching vibrations of the CH_2 group, respectively. The peak at 3060 cm^{-1} is attributed to C-H stretching vibration [82]. After the PDA-coating modification, the

absorption peaks appearing at 1631 cm^{-1} in the PDA@EPS samples are attributed to the N-H bending vibration [83], and the broad peak at 3424 cm^{-1} is associated with the stretching vibrations of the catechol -OH and N-H groups [84]. The presence of these characteristic peaks of PDA indicates the successful preparation of PDA@EPS particles.

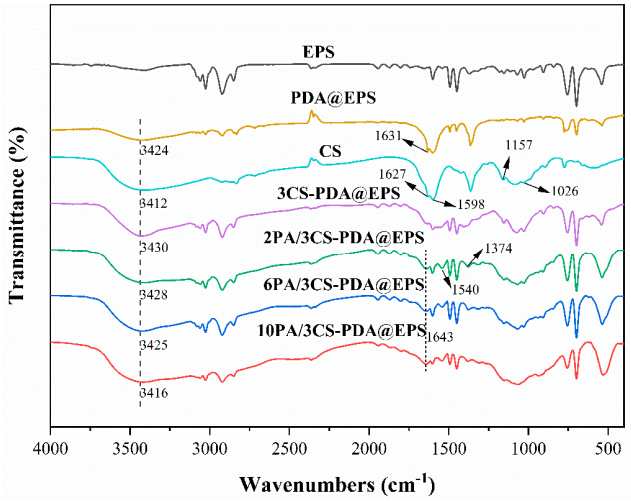

Figure 4. The FTIR spectra of different EPS samples.

In Figure 4, the peaks of CS at 1027 and 1157 cm^{-1} correspond to the C-O stretching vibration and the glycosidic bond (-C-O-C-) vibration, respectively [58]. The double peaks at 1598 cm^{-1} and 1627 cm^{-1} are bending vibrations of $-NH_2$ [85]. The broad band at 3419 cm^{-1} is around stretching vibrations of $-NH_2$ and -OH groups [86]. For 3CS-PDA@EPS, the changes in the peaks near 1072 and 1627 cm^{-1} indicate that the PDA@EPS particle surface was successfully coated with CS. After the PA-coating modification, the bending vibration peak of N-H in the PA/3CS-PDA@EPS samples is shifted to 1643 cm^{-1} due to the interaction between the amino group in CS and the phosphate group of PA [87,88]; the peak at 1374 cm^{-1} corresponds to the stretching vibration of P=O in PA [80,89]. The new peak at 1540 cm^{-1} is related to the complexation of PA and CS [59]. Compared with PDA@EPS, the O-H stretching vibrational bands of 3CS-PDA@EPS, 2PA/3CS-PDA@EPS, 6PA/3CS-PDA@EPS, and 10PA/3CS-PDA@EPS are shifted to 3430, 3428, 3425, and 3416 cm^{-1}, respectively, suggesting the existence of hydrogen bonding between PDA, CS, and PA [90]. Moreover, the peak of 3CS-PDA@EPS and PA/3CS-PDA@EPS becomes broader near 3400 cm^{-1}, indicating more amino group, hydroxyl group, and hydrogen bonding interactions in the modified EPS samples [58]. The elemental distribution of different EPS surfaces was analyzed by EDS (Figure S1). C (45.8 wt%), O (7 wt%), Na (4.5 wt%), N (1.1 wt%), and P (11.5 wt%) are uniformly distributed on the 10PA/3CS-PDA@EPS surface. In summary, the successful preparation of PA/3CS-PDA@EPS is achieved.

3.3. Water Contact Angle of EPS Samples

The WCA of the EPS foam board samples under different modification conditions is shown in Figure 5. The unmodified EPS sample is hydrophobic, with a WCA of 104.08°. After the introduction of PDA onto the EPS surface, the WCA of PDA@EPS is 22.18°, with good hydrophilicity, indicating that the PDA coating containing hydrophilic groups (-OH and -NH-) was successfully coated onto the EPS surface [57,91]. The surface of the EPS has been coated with CS and the WCA of the modified EPS samples is 83.2° after treatment, with a limited improvement in the hydrophilicity due to a certain degree of acetylation of CS (5%–15%) [74]. The WCA of the modified EPS samples is gradually decreased with increasing PA concentration, and the WCAs of the 2PA/3CS-PDA@EPS, 6PA/3CS-PDA@EPS, and 10PA/3CS-PDA@EPS samples are reduced to 75.14°, 64.3°, and 44.84°, respectively, which suggests that the phosphate groups in PA can effectively improve the

hydrophilicity of the samples [75], and this also proves that the increase in PA concentration leads to more phosphate groups adhering to the coating surface.

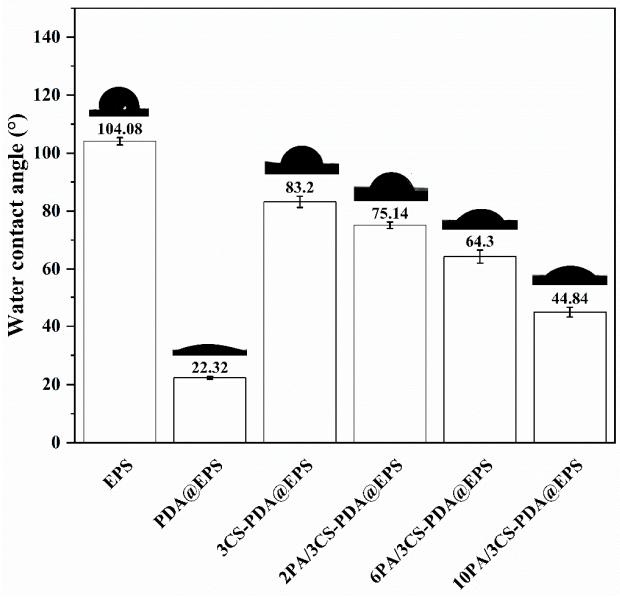

Figure 5. The water contact angles of different EPS samples.

3.4. Thermal Stability Properties of Eps Samples

The thermal stability of the EPS, PDA@EPS, CS-PDA@EPS, and PA/CS-PDA@EPS samples has been evaluated through TGA, and the results are shown in Figure 6 and Table 2. The TGA curve of expanded polystyrene indicates a clear, one-step thermal decomposition process with a maximum loss rate (DTG_{max}) of −1.88%/°C at 404 °C and almost no residue at 800 °C [82]. The thermal stability of PDA/EPS is improved compared to EPS, with a residual carbon content of 1.17 wt%. The presence of the PDA coating helps to trap the free carbon released from the EPS during the combustion process, promoting charring and preventing further pyrolysis of the EPS [51]. However, the thermal stability improvement is limited by the thin PDA coating on the PDA/EPS.

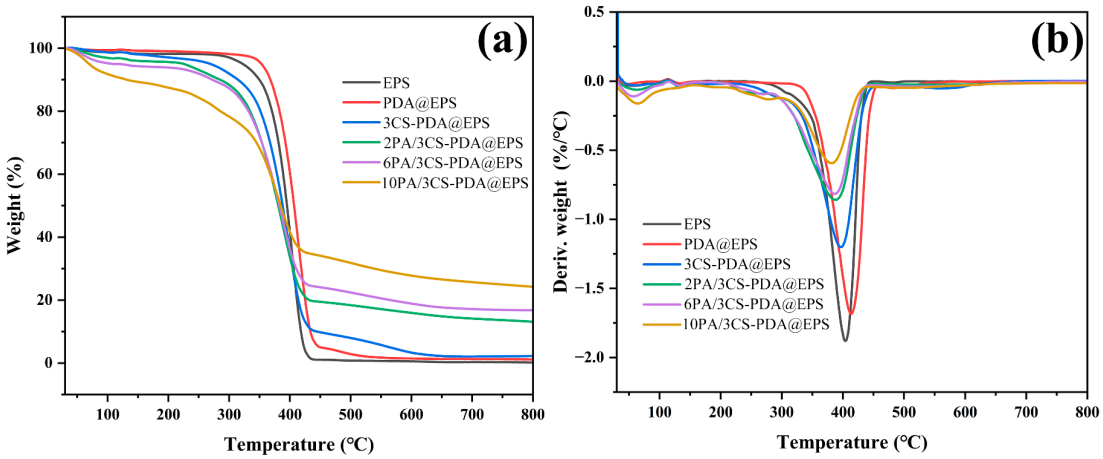

Figure 6. TG (**a**) and DTG (**b**) curves for different EPS samples.

In Figure 6, the thermal decomposition of 3CS-PDA@EPS in nitrogen occurs in three stages. In the first stage, from 30 °C to 180 °C, the mass loss is mainly attributed to the volatilization of free and bound water from CS and the decomposition of side chains [80]. In the second stage, from 240 °C–320 °C, the main chain of CS breaks, carbonation occurs, and non-flammable gas (water vapor, NH_3, and CO_2) is produced from decomposition [84].

The third stage is from 320 °C to 490 °C, which is mainly the continuous pyrolysis of the EPS. Thermal decomposition from 490 °C to 800 °C occurs when the high temperature destroys the charred protective layer of CS, exposing the internal polymer to the flame and causing additional thermal decomposition. The residual carbon content of 3CS-PDA@EPS is 2.23 wt%. The DTGmax is decreased to −1.2%/°C due to the formation of hydrogen bonds between PDA and CS, and thermal stability is improved [58,85]. The lower thermal stability of CS results in lower $T_{10\%}$, $T_{50\%}$, and T_{max} of CS-PDA@EPS [92].

Table 2. Thermal gravimetric analysis data of different EPS samples.

Sample	$T_{10\%}$ (°C)	$T_{50\%}$ (°C)	T_{max} (°C)	DTG_{max} (%/°C)	Residue (wt%) at 800 °C
EPS	350	395	404	−1.88	0.17
PDA@EPS	368	407	414	−1.68	1.11
3CS-PDA@EPS	314	388	396	−1.2	2.23
2PA/3CS-PDA@EPS	285	381	397	−0.86	13.1
6PA/3CS-PDA@EPS	273	383	386	−0.8	16.76
10PA/3CS-PDA@EPS	132	385	381	−0.59	24.19

$T_{10\%}$, $T_{50\%}$, and T_{max} correspond to temperatures with mass loss rates of 10% and 50% and a maximum mass loss rate, respectively.

The thermal decomposition curves of PA/3CS-PDA@EPS in nitrogen are similar to those of 3CS-PDA@EPS, but $T_{10\%}$, $T_{50\%}$, and T_{max} are reduced, which are related to the low thermal stability of PA/CS [73]. The thermal decomposition of PA at lower temperatures produces acidic substances such as phosphate, which promotes the dehydration reaction of CS and the formation of a carbon layer. Additionally, the ammonia produced by the decomposition of amino groups in CS causes the carbon layer to expand, and this expanded carbon layer improves the high-temperature thermal stability of PA/3CS-PDA@EPS [92]. Furthermore, the modified EPS demonstrates an increased ability to form carbon as the PA content increases. In comparison to the 3CS-PDA@EPS sample, the 2PA/3CS-PDA@EPS, 6PA/3CS-PDA@EPS, and 10PA/3CS-PDA@EPS samples exhibit a residual carbon content of 13.1 wt%, 16.76 wt%, and 24.19 wt%, respectively. The rise in residual carbon content is linked to the increase in the weight of the sample itself following PA modification. However, related studies have demonstrated that PA itself does not possess a significant carbon-forming capacity [59,76]. Consequently, the rise in residual carbon content can be attributed to PA facilitating the dehydration of CS to form carbon, with a high content of PA exhibiting a more pronounced effect [64,93]. Meanwhile, the DTG_{max} of the EPS samples modified with PA is reduced to −0.86%/°C, −0.8%/°C, and −0.59%/°C, respectively. With the formation of more carbon, the barrier of the carbon layer can provide better protection, effectively preventing further thermal decomposition of the EPS and improving the flame-retardant properties of the modified EPS [64,89,93].

3.5. Flammability Test of EPS Samples

In Figure 7, the unmodified EPS particles appear white, the PDA@EPS particles have a brown appearance, and the 3CS-PDA@EPS and 10PA/3CS-PDA@EPS particles have a darker brown color; the macro changes indicate successful preparation of modified EPS particles. In flammability tests of the EPS samples using a butane torch, the honeycomb structure of EPS rapidly shrinks when exposed to the flame, causing the particles to melt and leave a sticky residue (see Video S1). At high temperatures, EPS undergoes thermal decomposition, releasing volatile styrene monomers and oligomers, which burn rapidly and produce large amounts of smoke as the concentration of flammable gases increases at an ignition temperature of 350 °C [10,94]. The thin PDA coating on the surface of the EPS particles does not function as a flame retardant, and the PDA@EPS sample burns rapidly under a butane flame, producing large amounts of smoke and leaving behind a molten

polymer (see Video S2). For 3CS-PDA@EPS, some residual carbon is produced during combustion, which prevents the flame from spreading rapidly [46]. In Figure 7d1–d5, the flame spread of 10PA/3CS-PDA@EPS during combustion is significantly slower, smoke production is reduced, and a large amount of expanding residual carbon remains (see Video S4). The fire resistance effect of the PA/CS coatings may be responsible for this [65,72]. When undergoing thermal decomposition, PA facilitates the dehydration of CS into char and releases non-combustible ammonia and water vapor, which form an expanded char layer that acts as a protective barrier. Additionally, the non-combustible gases dilute the oxygen concentration. Combined with the TGA results, it can be assumed that the PA/CS-PDA@EPS particles have some degree of fire resistance.

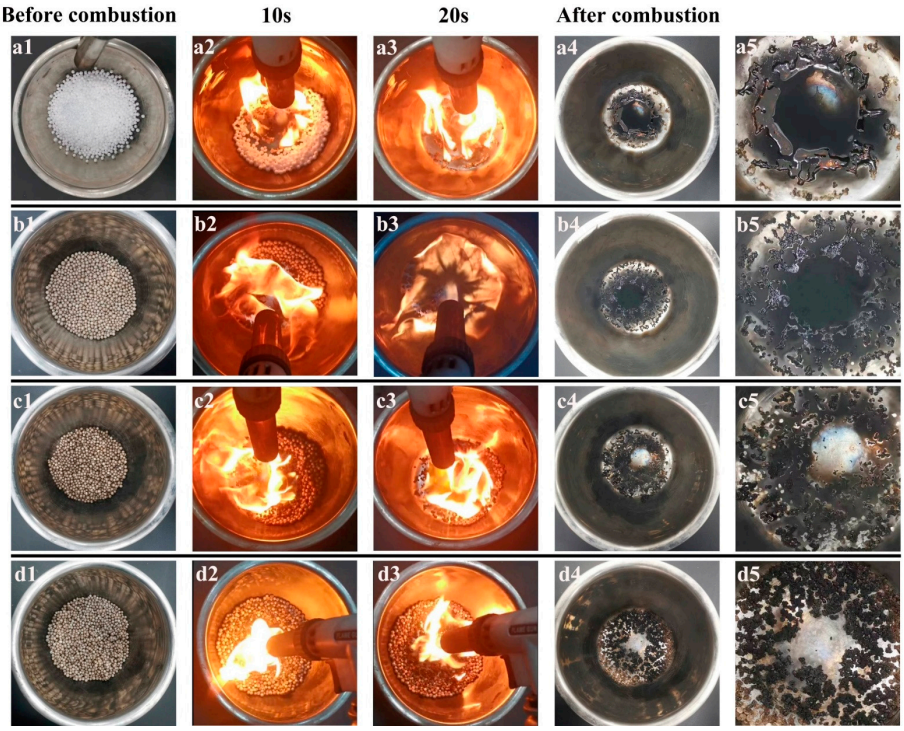

Figure 7. Flammability test of EPS (**a1**–**a5**), PDA@EPS (**b1**–**b5**), 3CS-PDA@EPS (**c1**–**c5**), and 10PA/3CS-PDA@EPS (**d1**–**d5**).

3.6. Water Resistance Test of EPS Samples

The change in mass of the modified EPS particles following multiple washes with tap water is illustrated in Figure 8A. All of the modified EPS particles show significant mass loss after the initial water washing. The 3CS-PDA@EPS samples exhibit an 11.76% reduction in mass following the initial water washing. However, there is minimal change in mass following multiple washes, indicating that the catechol groups in the PDA coating provided excellent adhesion and successfully immobilized the CS on the EPS surface. The 2PA/3CS-PDA@EPS samples exhibit the lowest mass loss (7.94%) and demonstrate good water resistance. This suggests that complex precipitation occurs between PA and CS through strong ionic interactions, which can improve the stability of the modified films [72]. The modified EPS samples with a high PA content have a high mass loss rate after multiple washes, which is attributed to the fact that PA only adheres to the coating surface by means of physical action. As illustrated in Figure 8B, the 10PA/3CS-PDA@EPS samples subjected to five cycles of water washing demonstrate a certain degree of fire resistance in the butane flame. Furthermore, the flame spreading speed slows down during the combustion process, forming expanding residual carbon.

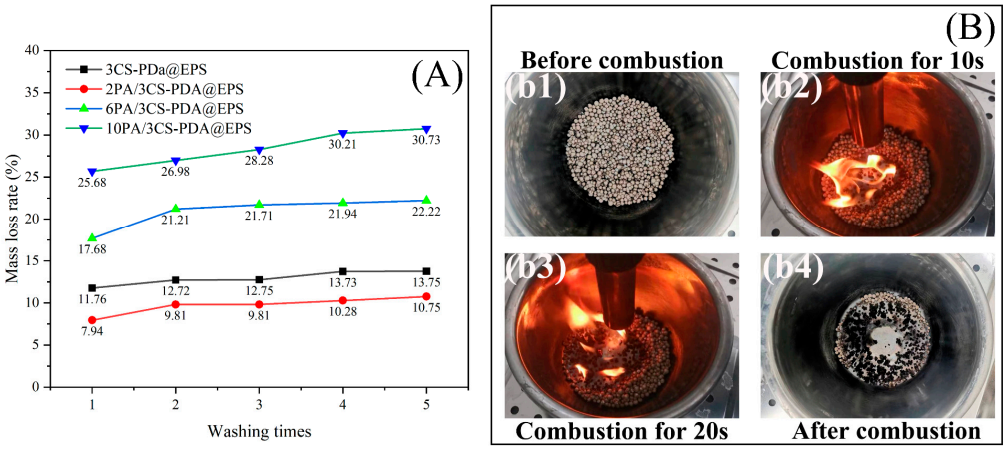

Figure 8. Water resistance test of EPS (**A**) and flammability test of 10PA/3CS-PDA@EPS by washing with tap water 5 times (**B**, **b1**–**b4**).

4. Conclusions

In this study, a bio-based coating was applied to modified EPS particles by using a simple coating method to address the hydrophobicity and flammability of EPS particles. PDA was used as an adhesive and the PA/CS IFR system was introduced onto the PDA@EPS particles through electrostatic self-organization. The PA/CS-PDA@EPS particles were prepared using the coating bio-based flame retardant method. The hydrophilicity of the modified EPS was enhanced compared to the unmodified EPS. The WCA on the surface of 10PA/3CS-PDA@EPS was measured to be 44.84°. TGA revealed that PA promotes an improvement in carbon formation and in the thermal stability of the modified EPS particles. The residual carbon contents of the 2PA/3CS-PDA@EPS, 6PA/3CS-PDA@EPS, and 10PA/3CS-PDA@EPS samples were 13.1 wt%, 16.76 wt%, and 24.19 wt% respectively, corresponding to a decrease in the DTG_{max} from −1.88 to −0.86%/°C, −0.8%/°C, and −0.59%/°C respectively. The butane combustion test demonstrated that the 10PA/3CS-PDA@EPS samples exhibited flame-retardant properties and remained fire resistant following multiple water washes. Thus, flame-retardant and hydrophilic EPS particles are expected to have wider applications.

Supplementary Materials: The following supporting information can be downloaded at: https://www.mdpi.com/article/10.3390/coatings14050574/s1, Figure S1: Elemental mapping (N, Na, and P elements) of modified-EPS particles recorded with SEM-EDS, Video S1: Flame-retardant testing of EPS particles; Video S2: Flame-retardant testing of PDA@EPS particles; Video S3: Flame-retardant testing of 3CS-PDA@EPS particles; Video S4: Flame-retardant testing of 10PA/3CS-PDA@EPS particles.

Author Contributions: Conceptualization, W.T.; methodology, W.T.; software, W.L.; validation, W.L.; formal analysis, W.T., D.H. and W.L.; investigation, W.T.; resources, D.H. and X.Q.; data curation, W.T.; writing—original draft preparation, W.T.; writing—review and editing, D.H.; supervision, D.H. and X.Q.; project administration, D.H.; funding acquisition, D.H. and X.Q. All authors have read and agreed to the published version of the manuscript.

Funding: This study was funded by [the Science and Technology Planning Project of Nature Science Foundation of the Gansu Province, China], grant number [No. 21JR7RA279], [the Science and Technology Major Project of the Gansu Province], grant number [No. 22ZD6GD062], and [the Science and Technology Project of Open Subject of Attapulgite Industry in Linze County], grant number [No. LZKFKT-2103].

Institutional Review Board Statement: Not applicable.

Informed Consent Statement: Not applicable.

Data Availability Statement: The data for this paper are available from the authors upon reasonable request.

Conflicts of Interest: The authors declare no conflict of interest.

References

1. Berardi, U. A cross-country comparison of the building energy consumptions and their trends. *Resour. Conserv. Recycl.* **2017**, *123*, 230–241. [CrossRef]
2. Huang, Y.; Niu, J.L.; Chung, T.M. Study on performance of energy-efficient retrofitting measures on commercial building external walls in cooling-dominant cities. *Appl. Energy* **2013**, *103*, 97–108. [CrossRef]
3. Shi, J.Y.; Liu, B.J.; Liu, Y.C.; Wang, E.L.; He, Z.H.; Xu, H.J.; Ren, X.D. Preparation and characterization of lightweight aggregate foamed geopolymer concretes aerated using hydrogen peroxide. *Constr. Build. Mater.* **2020**, *256*, 119442. [CrossRef]
4. Rashad, A.M.; Mosleh, Y.A.; Mokhtar, M.M. Thermal insulation and durability of alkali-activated lightweight slag mortar modified with silica fume and fly ash. *Constr. Build. Mater.* **2024**, *411*, 134255. [CrossRef]
5. Cavalline, T.L.; Gallegos, J.; Castrodale, R.W.; Freeman, C.; Liner, J.; Wall, J. Influence of Lightweight Aggregate Concrete Materials on Building Energy Performance. *Buildings* **2021**, *11*, 94. [CrossRef]
6. Aditya, L.; Mahlia, T.M.I.; Rismanchi, B.; Ng, H.M.; Hasan, M.H.; Metselaar, H.S.C.; Muraza, O.; Aditiya, H.B. A review on insulation materials for energy conservation in buildings. *Renew. Sustain. Energy Rev.* **2017**, *73*, 1352–1365. [CrossRef]
7. Hung Anh, L.D.; Pásztory, Z. An overview of factors influencing thermal conductivity of building insulation materials. *J. Build. Eng.* **2021**, *44*, 102604. [CrossRef]
8. Bouzit, S.; Merli, F.; Sonebi, M.; Buratti, C.; Taha, M. Gypsum-plasters mixed with polystyrene balls for building insulation: Experimental characterization and energy performance. *Constr. Build. Mater.* **2021**, *283*, 122625. [CrossRef]
9. Sayadi, A.A.; Tapia, J.V.; Neitzert, T.R.; Clifton, G.C. Effects of expanded polystyrene (EPS) particles on fire resistance, thermal conductivity and compressive strength of foamed concrete. *Constr. Build. Mater.* **2016**, *112*, 716–724. [CrossRef]
10. Mehta, S.; Biederman, S.; Shivkumar, S. Thermal-Degradation of Foamed Polystyrene. *J. Mater. Sci.* **1995**, *30*, 2944–2949. [CrossRef]
11. Xu, Q.; Jin, C.; Griffin, G.; Jiang, Y. Fire safety evaluation of expanded polystyrene foam by multi-scale methods. *J. Therm. Anal. Calorim.* **2013**, *115*, 1651–1660. [CrossRef]
12. Jin, Z.; Ma, B.; Su, Y.; Qi, H.; Lu, W.; Zhang, T. Preparation of eco-friendly lightweight gypsum: Use of beta-hemihydrate phosphogypsum and expanded polystyrene particles. *Constr. Build. Mater.* **2021**, *297*, 123837. [CrossRef]
13. Huang, J.; Zhao, Z.; Chen, T.; Zhu, Y.; Lv, Z.; Gong, X.; Niu, Y.; Ma, B. Preparation of highly dispersed expandable graphite/polystyrene composite foam via suspension polymerization with enhanced fire retardation. *Carbon* **2019**, *146*, 503–512. [CrossRef]
14. Hamdani-Devarennes, S.; El Hage, R.; Dumazert, L.; Sonnier, R.; Ferry, L.; Lopez-Cuesta, J.M.; Bert, C. Water-based flame retardant coating using nano-boehmite for expanded polystyrene (EPS) foam. *Prog. Org. Coat.* **2016**, *99*, 32–46. [CrossRef]
15. Wang, Y.C.; Zhao, J.P. Comparative study on flame retardancy of silica fume-based geopolymer activated by different activators. *J. Alloys Compd.* **2018**, *743*, 108–114. [CrossRef]
16. Gheonea, R.; Crasmareanu, E.C.; Plesu, N.; Sauca, S.; Simulescu, V.; Ilia, G. New Hybrid Materials Synthesized with Different Dyes by Sol-Gel Method. *Adv. Mater. Sci. Eng.* **2017**, *2017*, 4537039. [CrossRef]
17. Vahabi, H.; Gholami, F.; Tomas, M.; Movahedifar, E.; Yazdi, M.K.; Saeb, M.R. Hydrogel and aerogel-based flame-retardant polymeric materials: A review. *J. Vinyl Addit. Technol.* **2024**, *30*, 5–25. [CrossRef]
18. Chen, M.; Tang, M.Q.; Qi, F.; Chen, X.L.; He, W.D. Microencapsulated ammonium polyphosphate and its application in the flame retardant polypropylene composites. *J. Fire Sci.* **2015**, *33*, 374–389. [CrossRef]
19. Guo, W.W.; Wang, X.; Zhang, P.; Liu, J.J.; Song, L.; Hu, Y. Nano-fibrillated cellulose-hydroxyapatite based composite foams with excellent fire resistance. *Carbohydr. Polym.* **2018**, *195*, 71–78. [CrossRef]
20. Varnagiris, S.; Tuckute, S.; Lelis, M.; Milcius, D. SiO2 films as heat resistant layers for protection of expandable polystyrene foam from flame torch-induced heat. *J. Thermoplast. Compos. Mater.* **2018**, *31*, 657–667. [CrossRef]
21. Zhang, J.; Liu, B.W.; Zhou, Y.X.; Essawy, H.; Zhao, C.L.; Wu, Z.G.; Zhou, X.J.; Hou, D.F.; Du, G.B. Gelatinized starch-furanic hybrid as a biodegradable thermosetting resin for fabrication of foams for building materials. *Carbohydr. Polym.* **2022**, *298*, 120157. [CrossRef] [PubMed]
22. Ji, W.; Wang, D.; Guo, J.; Fei, B.; Gu, X.; Li, H.; Sun, J.; Zhang, S. The preparation of starch derivatives reacted with urea-phosphoric acid and effects on fire performance of expandable polystyrene foams. *Carbohydr. Polym.* **2020**, *233*, 115841. [CrossRef] [PubMed]
23. Li, M.-E.; Yan, Y.-W.; Zhao, H.-B.; Jian, R.-K.; Wang, Y.-Z. A facile and efficient flame-retardant and smoke-suppressant resin coating for expanded polystyrene foams. *Compos. Part B* **2020**, *185*, 107797. [CrossRef]
24. Cao, B.; Yu, T.; Sun, J.; Gu, X.Y.; Liu, X.D.; Li, H.F.; Fei, B.; Zhang, S. Improving the fire performance and smoke suppression of expandable polystyrene foams by coating with multi-dimensional carbon nanoparticles. *J. Appl. Polym. Sci.* **2020**, *137*, 49227. [CrossRef]
25. Wang, L.Y.; Wang, C.; Liu, P.W.; Jing, Z.J.; Ge, X.S.; Jiang, Y.J. The flame resistance properties of expandable polystyrene foams coated with a cheap and effective barrier layer. *Constr. Build. Mater.* **2018**, *176*, 403–414. [CrossRef]
26. Jia, Y.; Luo, B.; Lee, S.H.; Huang, H.; Wu, Z.; Zhou, B.; Zhou, X.; Zhang, J. Facile preparation of high-performance plywood adhesive from gelatinized corn starch crosslinked with ammonium dihydrogen phosphate. *Int. J. Biol. Macromol.* **2024**, *256*, 128548. [CrossRef]
27. Takigami, H.; Watanabe, M.; Kajiwara, N. Destruction behavior of hexabromocyclododecanes during incineration of solid waste containing expanded and extruded polystyrene insulation foams. *Chemosphere* **2014**, *116*, 24–33. [CrossRef]

28. Hou, M.M.; Wang, Y.; Zhao, H.X.; Zhang, Q.N.; Xie, Q.; Zhang, X.J.; Chen, R.Z.; Chen, J.W. Halogenated flame retardants in building and decoration materials in China: Implications for human exposure via inhalation and dust ingestion. *Chemosphere* **2018**, *203*, 291–299. [CrossRef]
29. van der Veen, I.; de Boer, J. Phosphorus flame retardants: Properties, production, environmental occurrence, toxicity and analysis. *Chemosphere* **2012**, *88*, 1119–1153. [CrossRef]
30. Huo, S.Q.; Song, P.A.; Yu, B.; Ran, S.Y.; Chevali, V.S.; Liu, L.; Fang, Z.P.; Wang, H. Phosphorus-containing flame retardant epoxy thermosets: Recent advances and future perspectives. *Prog. Polym. Sci.* **2021**, *114*, 101366. [CrossRef]
31. Ji, W.F.; Yao, Y.; Guo, J.; Fei, B.; Gu, X.Y.; Li, H.F.; Sun, J.; Zhang, S. Toward an understanding of how red phosphorus and expandable graphite enhance the fire resistance of expandable polystyrene foams. *J. Appl. Polym. Sci.* **2020**, *137*, 49045. [CrossRef]
32. Yan, Y.W.; Huang, J.Q.; Guan, Y.H.; Shang, K.; Jian, R.K.; Wang, Y.Z. Flame retardance and thermal degradation mechanism of polystyrene modified with aluminum hypophosphite. *Polym. Degrad. Stab.* **2014**, *99*, 35–42. [CrossRef]
33. Shao, X.M.; Du, Y.Q.; Zheng, X.F.; Wang, J.C.; Wang, Y.C.; Zhao, S.; Xin, Z.X.; Li, L. Reduced fire hazards of expandable polystyrene building materials via intumescent flame-retardant coatings. *J. Mater. Sci.* **2020**, *55*, 7555–7572. [CrossRef]
34. Chindaprasirt, P.; Hiziroglu, S.; Waisurasingha, C.; Kasemsiri, P. Properties of Wood Flour/Expanded Polystyrene Waste Composites Modified With Diammonium Phosphate Flame Retardant. *Polym. Compos.* **2015**, *36*, 604–612. [CrossRef]
35. Laoutid, F.; Bonnaud, L.; Alexandre, M.; Lopez-Cuesta, J.M.; Dubois, P. New prospects in flame retardant polymer materials: From fundamentals to nanocomposites. *Mater. Sci. Eng. R* **2009**, *63*, 100–125. [CrossRef]
36. Zhang, X.H.; Liu, F.; Chen, S.; Qi, G.R. Novel flame retardant thermosets from nitrogen-containing and phosphorus-containing epoxy resins cured with dicyandiamide. *J. Appl. Polym. Sci.* **2007**, *106*, 2391–2397. [CrossRef]
37. Wang, N.; Liu, Y.S.; Liu, Y.; Wang, Q. Properties and mechanisms of different guanidine flame retardant wood pulp paper. *J. Anal. Appl. Pyrolysis* **2017**, *128*, 224–231. [CrossRef]
38. Ruan, C.P.; Ai, K.L.; Li, X.B.; Lu, L.H. A Superhydrophobic Sponge with Excellent Absorbency and Flame Retardancy. *Angew. Chem. Int. Ed.* **2014**, *53*, 5556–5560. [CrossRef]
39. Chen, M.J.; Shao, Z.B.; Wang, X.L.; Chen, L.; Wang, Y.Z. Halogen-Free Flame-Retardant Flexible Polyurethane Foam with a Novel Nitrogen-Phosphorus Flame Retardant. *Ind. Eng. Chem. Res.* **2012**, *51*, 9769–9776. [CrossRef]
40. Castellano, A.; Colleoni, C.; Iacono, G.; Mezzi, A.; Plutino, M.R.; Malucelli, G.; Rosace, G. Synthesis and characterization of a phosphorous/nitrogen based sol-gel coating as a novel halogen- and formaldehyde-free flame retardant finishing for cotton fabric. *Polym. Degrad. Stab.* **2019**, *162*, 148–159. [CrossRef]
41. Zhu, Z.M.; Xu, Y.J.; Liao, W.; Xu, S.M.; Wang, Y.Z. Highly Flame Retardant Expanded Polystyrene Foams from Phosphorus-Nitrogen-Silicon Synergistic Adhesives. *Ind. Eng. Chem. Res.* **2017**, *56*, 4649–4658. [CrossRef]
42. Maqsood, M.; Seide, G. Biodegradable Flame Retardants for Biodegradable Polymer. *Biomolecules* **2020**, *10*, 1038. [CrossRef] [PubMed]
43. Liu, Y.; Zhang, A.; Cheng, Y.; Li, M.; Cui, Y.; Li, Z. Recent advances in biomass phytic acid flame retardants. *Polym. Test.* **2023**, *124*, 108100. [CrossRef]
44. Taib, M.; Antov, P.; Savov, V.; Fatriasari, W.; Madyaratri, E.W.; Wirawan, R.; Osvaldová, L.M.; Hua, L.S.; Ghani, M.A.A.; Al Edrus, S.; et al. Current progress of biopolymer-based flame retardant. *Polym. Degrad. Stab.* **2022**, *205*, 110153. [CrossRef]
45. Zhang, S.; Liu, X.; Jin, X.; Li, H.; Sun, J.; Gu, X. The novel application of chitosan: Effects of cross-linked chitosan on the fire performance of thermoplastic polyurethane. *Carbohydr. Polym.* **2018**, *189*, 313–321. [CrossRef] [PubMed]
46. Liu, X.; Gu, X.; Sun, J.; Zhang, S. Preparation and characterization of chitosan derivatives and their application as flame retardants in thermoplastic polyurethane. *Carbohydr. Polym.* **2017**, *167*, 356–363. [CrossRef] [PubMed]
47. Guo, J.Z.; Wang, X.Y.; Li, Y.T.; Tan, S.M.; Zhao, S.; Li, L. Synthesis of bio-based toughening phosphorus-nitrogen flame retardant and study on high toughness EPS flame retardant insulation sheet. *Polym. Degrad. Stab.* **2023**, *218*, 110560. [CrossRef]
48. Qin, M.; Hu, X.; Guo, J. Preparation of a New Type of Expansion Flame Retardant and Application in Polystyrene. *Coatings* **2023**, *13*, 733. [CrossRef]
49. Nabipour, H.; Wang, X.; Song, L.; Hu, Y. A fully bio-based coating made from alginate, chitosan and hydroxyapatite for protecting flexible polyurethane foam from fire. *Carbohydr. Polym.* **2020**, *246*, 116641. [CrossRef]
50. Chen, H.B.; Shen, P.; Chen, M.J.; Zhao, H.B.; Schiraldi, D.A. Highly Efficient Flame Retardant Polyurethane Foam with Alginate/Clay Aerogel Coating. *ACS Appl. Mater. Interfaces* **2016**, *8*, 32557–32564. [CrossRef]
51. Cho, J.H.; Vasagar, V.; Shanmuganathan, K.; Jones, A.R.; Nazarenko, S.; Ellison, C.J. Bioinspired Catecholic Flame Retardant Nanocoating for Flexible Polyurethane Foams. *Chem. Mater.* **2015**, *27*, 6784–6790. [CrossRef]
52. Yang, W.; Wu, S.; Yang, W.; Chun-Yin Yuen, A.; Zhou, Y.; Yeoh, G.; Boyer, C.; Wang, C.H. Nanoparticles of polydopamine for improving mechanical and flame-retardant properties of an epoxy resin. *Compos. Part B* **2020**, *186*, 107828. [CrossRef]
53. Furtado, L.M.; Ando, R.A.; Petri, D.F.S. Polydopamine-coated cellulose acetate butyrate microbeads for caffeine removal. *J. Mater. Sci.* **2019**, *55*, 3243–3258. [CrossRef]
54. Huang, D.; Zheng, Y.; Quan, Q. Enhanced mechanical properties and UV shield of carboxymethyl cellulose films with polydopamine-modified natural fibre-like palygorskite. *Appl. Clay Sci.* **2019**, *183*, 105314. [CrossRef]
55. Yassin, M.A.; Gad, A.A.M. Immobilized Enzyme on Modified Polystyrene Foam Waste: A Biocatalyst for Wastewater Decolorization. *J. Environ. Chem. Eng.* **2020**, *8*, 104435. [CrossRef]

56. Jin, Z.; Xiao, Y.; Xu, Z.; Zhang, Z.; Wang, H.; Mu, X.; Gui, Z. Dopamine-modified poly(styrene) nanospheres as new high-speed adsorbents for copper-ions having enhanced smoke-toxicity-suppression and flame-retardancy. *J. Colloid Interface Sci.* **2021**, *582*, 619–630. [CrossRef] [PubMed]
57. Hecker, M.; Ting, M.S.H.; Malmström, J. Simple coatings to render polystyrene protein resistant. *Coatings* **2018**, *8*, 55. [CrossRef]
58. Huang, B.-H.; Li, S.-Y.; Chiou, Y.-J.; Chojniak, D.; Chou, S.-C.; Wong, V.C.M.; Chen, S.-Y.; Wu, P.-W. Electrophoretic fabrication of a robust chitosan/polyethylene glycol/polydopamine composite film for UV-shielding application. *Carbohydr. Polym.* **2021**, *273*, 118560. [CrossRef] [PubMed]
59. Stephy, A.; Antony, A.M.; Francis, T. Thermal Degradation Kinetics of Chitosan/Phytic Acid Polyelectrolyte Complex as Investigated by Thermogravimetric Analysis. *J. Appl. Polym. Sci.* **2023**, *31*, 210–220. [CrossRef]
60. Deak, N.A.; Johnson, L.A. Fate of phytic acid in producing soy protein ingredients. *J. Am. Oil Chem. Soc.* **2007**, *84*, 369–376. [CrossRef]
61. Sim, G.Y.; Lee, S.U.; Lee, J.W. Enhanced extraction of phytic acid from rice hulls with enzymatic treatment and production of ethanol from reducing sugars in hydrolyzed rice hulls after extraction of phytic acid. *Lwt-Food Sci. Technol.* **2020**, *133*, 110111. [CrossRef]
62. Bloot, A.P.M.; Kalschne, D.L.; Amaral, J.A.S.; Baraldi, I.J.; Canan, C. A Review of Phytic Acid Sources, Obtention, and Applications. *Food Rev. Int.* **2023**, *39*, 73–92. [CrossRef]
63. Cheng, X.W.; Guan, J.P.; Yang, X.H.; Tang, R.C.; Yao, F. A bio-resourced phytic acid/chitosan polyelectrolyte complex for the flame retardant treatment of wool fabric. *J. Clean. Prod.* **2019**, *223*, 342–349. [CrossRef]
64. Li, M.-E.; Zhao, H.-B.; Cheng, J.-B.; Wang, T.; Fu, T.; Zhang, A.-N.; Wang, Y.-Z. An Effective Green Porous Structural Adhesive for Thermal Insulating, Flame-Retardant, and Smoke-Suppressant Expandable Polystyrene Foam. *Engineering* **2022**, *17*, 151–160. [CrossRef]
65. Laufer, G.; Kirkland, C.; Morgan, A.B.; Grunlan, J.C. Intumescent multilayer nanocoating, made with renewable polyelectrolytes, for flame-retardant cotton. *Biomacromolecules* **2012**, *13*, 2843–2848. [CrossRef]
66. van den Broek, L.A.; Knoop, R.J.; Kappen, F.H.; Boeriu, C.G. Chitosan films and blends for packaging material. *Carbohydr. Polym.* **2015**, *116*, 237–242. [CrossRef] [PubMed]
67. Sivanesan, I.; Gopal, J.; Muthu, M.; Shin, J.; Mari, S.; Oh, J. Green Synthesized Chitosan/Chitosan Nanoforms/Nanocomposites for Drug Delivery Applications. *Polymers* **2021**, *13*, 2256. [CrossRef]
68. Rinaudo, M. Chitin and chitosan: Properties and applications. *Prog. Polym. Sci.* **2006**, *31*, 603–632. [CrossRef]
69. Riva, R.; Ragelle, H.; des Rieux, A.; Duhem, N.; Jérôme, C.; Préat, V. Chitosan and Chitosan Derivatives in Drug Delivery and Tissue Engineering. *Adv. Polym. Sci.* **2011**, *244*, 19–44.
70. Chen, C.; Gu, X.; Jin, X.; Sun, J.; Zhang, S. The effect of chitosan on the flammability and thermal stability of polylactic acid/ammonium polyphosphate biocomposites. *Carbohydr. Polym.* **2017**, *157*, 1586–1593. [CrossRef]
71. Lee, D.W.; Lim, H.; Chong, H.N.; Shim, W.S. Advances in chitosan material and its hybrid derivatives: A review. *Open Biomed. J.* **2009**, *1*, 10–20. [CrossRef]
72. Cheng, X.; Shi, L.; Fan, Z.; Yu, Y.; Liu, R. Bio-based coating of phytic acid, chitosan, and biochar for flame-retardant cotton fabrics. *Polym. Degrad. Stab.* **2022**, *199*, 109898. [CrossRef]
73. Fang, Y.; Sun, W.; Li, J.; Liu, H.; Liu, X. Eco-friendly flame retardant and dripping-resistant of polyester/cotton blend fabrics through layer-by-layer assembly fully bio-based chitosan/phytic acid coating. *Int. J. Biol. Macromol.* **2021**, *175*, 140–146. [CrossRef] [PubMed]
74. Spriano, S.; Riccucci, G.; Örlygsson, G.; Ng, C.H.; Vernè, E.; Sehn, F.P.; de Oliveira, P.T.; Ferraris, S. Coating of bioactive glasses with chitosan: The effects of the glass composition and coating method on the surface properties, including preliminary in vitro results. *Surf. Coat. Technol.* **2023**, *470*, 129824. [CrossRef]
75. Xie, L.; Liu, Y.; Zhang, W.; Xu, S. A dopamine/tannic-acid-based co-deposition combined with phytic acid modification to enhance the anti-fouling property of RO membrane. *Membranes* **2021**, *11*, 342. [CrossRef] [PubMed]
76. Liu, C.W.; Zhang, T.; Luo, Y.X.; Wang, Y.X.; Li, J.C.; Ye, T.; Guo, R.F.; Song, P.A.; Zhou, J.; Wang, H. Multifunctional polyurethane sponge coatings with excellent flame retardant, antibacterial, compressible, and recyclable properties. *Compos. Part B* **2021**, *215*, 108785. [CrossRef]
77. Xu, B.T.; Jin, D.Z.; Yu, Y.; Zhang, Q.; Weng, W.J.; Ren, K.X.; Tai, Y.L. Nanoclay-reinforced alginate aerogels: Preparation and properties. *Rsc Adv.* **2024**, *14*, 954–962. [CrossRef] [PubMed]
78. Chen, M.J.; Lazar, S.; Kolibaba, T.J.; Shen, R.Q.; Quan, Y.F.; Wang, Q.S.; Chiang, H.C.; Palen, B.; Grunlan, J.C. Environmentally Benign and Self-Extinguishing Multilayer Nanocoating for Protection of Flammable Foam. *ACS Appl. Mater. Interfaces* **2020**, *12*, 49130–49137. [CrossRef]
79. Gonçalves, O.H.; Leimann, F.V.; de Araújo, P.H.H.; Machado, R.A.F. Expansion of core–shell PS/PMMA particles. *J. Appl. Polym. Sci.* **2013**, *130*, 4521–4527. [CrossRef]
80. Han, D.; Zhao, H.; Gao, L.; Qin, Z.; Ma, J.; Han, Y.; Jiao, T. Preparation of carboxymethyl chitosan/phytic acid composite hydrogels for rapid dye adsorption in wastewater treatment. *Colloids Surf. A* **2021**, *628*, 127355. [CrossRef]
81. Li, S.; Zhao, F.; Wang, X.; Liu, Z.; Guo, J.; Li, Y.; Tan, S.; Xin, Z.; Zhao, S.; Li, L. A green flame retardant coating based on one-step aqueous complexation of phytic acid and urea for fabrication of lightweight and high toughness flame retardant EPS insulation board. *Polym. Degrad. Stab.* **2024**, *219*, 110597. [CrossRef]

82. Bhoite, S.P.; Kim, J.; Jo, W.; Bhoite, P.H.; Mali, S.S.; Park, K.H.; Hong, C.K. Expanded Polystyrene Beads Coated with Intumescent Flame Retardant Material to Achieve Fire Safety Standards. *Polymers* **2021**, *13*, 2662. [CrossRef] [PubMed]
83. Lin, C.; Fu, J.; Liu, S. Facile preparation of Au nanoparticle-embedded polydopamine hollow microcapsule and its catalytic activity for the reduction of methylene blue. *J. Macromol. Sci. Part A Pure Appl. Chem.* **2019**, *56*, 1104–1113. [CrossRef]
84. MohammadAlizadeh, A.; Elmi, F. Flame retardant and superoleophilic polydopamine/chitosan-graft (g)-octanal coated polyurethane foam for separation oil/water mixtures. *Int. J. Biol. Macromol.* **2024**, *259*, 129237. [CrossRef] [PubMed]
85. Liao, Y.; Wang, M.; Chen, D. Preparation of polydopamine-modified graphene oxide/chitosan aerogel for uranium (VI) adsorption. *Ind. Eng. Chem. Res.* **2018**, *57*, 8472–8483. [CrossRef]
86. Han, G.; Liu, S.; Pan, Z.; Lin, Y.; Ding, S.; Li, L.; Luo, B.; Jiao, Y.; Zhou, C. Sulfonated chitosan and phosphorylated chitosan coated polylactide membrane by polydopamine-assisting for the growth and osteogenic differentiation of MC3T3-E1s. *Carbohydr. Polym.* **2020**, *229*, 115517. [CrossRef]
87. Qi, L.; Xu, Z.; Jiang, X.; Hu, C.; Zou, X. Preparation and antibacterial activity of chitosan nanoparticles. *Carbohydr. Res.* **2004**, *339*, 2693–2700. [CrossRef]
88. Omar, H.; Fardous, R.; Alhindi, Y.M.; Aodah, A.H.; Alyami, M.; Alsuabeyl, M.S.; Alghamdi, W.M.; Alhasan, A.H.; Almalik, A. α1-acid glycoprotein-decorated hyaluronic acid nanoparticles for suppressing metastasis and overcoming drug resistance breast cancer. *Biomedicines* **2022**, *10*, 414. [CrossRef] [PubMed]
89. Liu, Z.H.; Song, S.K.; Dong, L.B.; Guo, J.Z.; Wang, J.C.; Tan, S.M.; Li, Y.T.; Shen, M.; Zhao, S.; Li, L.; et al. Bio-based phytic acid and urea interfacial layer by layer assembly for flame-retardant cotton. *Polym. Degrad. Stab.* **2023**, *216*, 110479. [CrossRef]
90. Zhang, L.; Li, Z.; Pan, Y.T.; Yáñez, A.P.; Hu, S.; Zhang, X.Q.; Wang, R.; Wang, D.Y. Polydopamine induced natural fiber surface functionalization: A way towards flame retardancy of flax/poly(lactic acid) biocomposites. *Compos. Part B* **2018**, *154*, 56–63. [CrossRef]
91. Jiang, J.; Zhu, L.; Zhu, L.; Zhang, H.; Zhu, B.; Xu, Y. Antifouling and antimicrobial polymer membranes based on bioinspired polydopamine and strong hydrogen-bonded poly (N-vinyl pyrrolidone). *ACS Appl. Mater. Interfaces* **2013**, *5*, 12895–12904. [CrossRef] [PubMed]
92. Kumar Kundu, C.; Wang, W.; Zhou, S.; Wang, X.; Sheng, H.; Pan, Y.; Song, L.; Hu, Y. A green approach to constructing multilayered nanocoating for flame retardant treatment of polyamide 66 fabric from chitosan and sodium alginate. *Carbohydr. Polym.* **2017**, *166*, 131–138. [CrossRef] [PubMed]
93. Cheng, X.W.; Guan, J.P.; Tang, R.C.; Liu, K.Q. Phytic acid as a bio-based phosphorus flame retardant for poly(lactic acid) nonwoven fabric. *J. Clean. Prod.* **2016**, *124*, 114–119. [CrossRef]
94. Faravelli, T.; Pinciroli, M.; Pisano, F.; Bozzano, G.; Dente, M.; Ranzi, E. Thermal degradation of polystyrene. *J. Anal. Appl. Pyrolysis* **2001**, *60*, 103–121. [CrossRef]